Supporting Information for:

TLR4 blockade using docosahexaenoic acid restores vulnerability of drug-tolerant tumor cells and prevents breast cancer metastasis and post-surgical relapse

Mou Wang[a,†], Yuejing Wang[a,†], Renhe Liu[b,d], Ruilian Yu[c], Tao Gong[a], Zhirong Zhang[a] , Yao Fu[a*]

[a] Key Laboratory of Drug-Targeting and Drug Delivery System of the Education Ministry and Sichuan Province, Sichuan Engineering Laboratory for Plant-Sourced Drug and Sichuan Research Center for Drug Precision Industrial Technology, West China School of Pharmacy, Sichuan University, Chengdu 610041, China.

[b] The Scripps Research Institute, 10550 N. Torrey Pines Road, La Jolla, CA 92037, USA.

[c] Department of Oncology, Sichuan Provincial Key Laboratory for Human Disease Gene Study, Sichuan Provincial People's Hospital, University of Electronic Science and Technology of China, Chengdu 610072, China.

[d] Current address: Global Health Drug Discovery Institute, Beijing 100084, China.

[†] These authors made equal contributions to this work.

[*]Corresponding authors.

Emails: yfu4@scu.edu.cn (Yao. Fu).

Study design

The primary objective of this study was to evaluate the therapeutic efficacy of the combination of DOX and DHA against breast cancer metastasis and postsurgical relapse. We evaluated the response to DHA-only or in combination with conventional chemotherapy (DOX) in mouse 4T1 cells in vitro and 4T1 orthotopic or experimental metastasis models in vivo. All mice were randomly divided into saline, DOX-only solution, DHA-only solution, DOX + DHA solution, and DOX/DHA-LNs groups. The numbers of replicates performed for each experiment are included in the figure legends. Experiments were designed to investigate the mechanisms of antitumor and anti-metastasis effect.

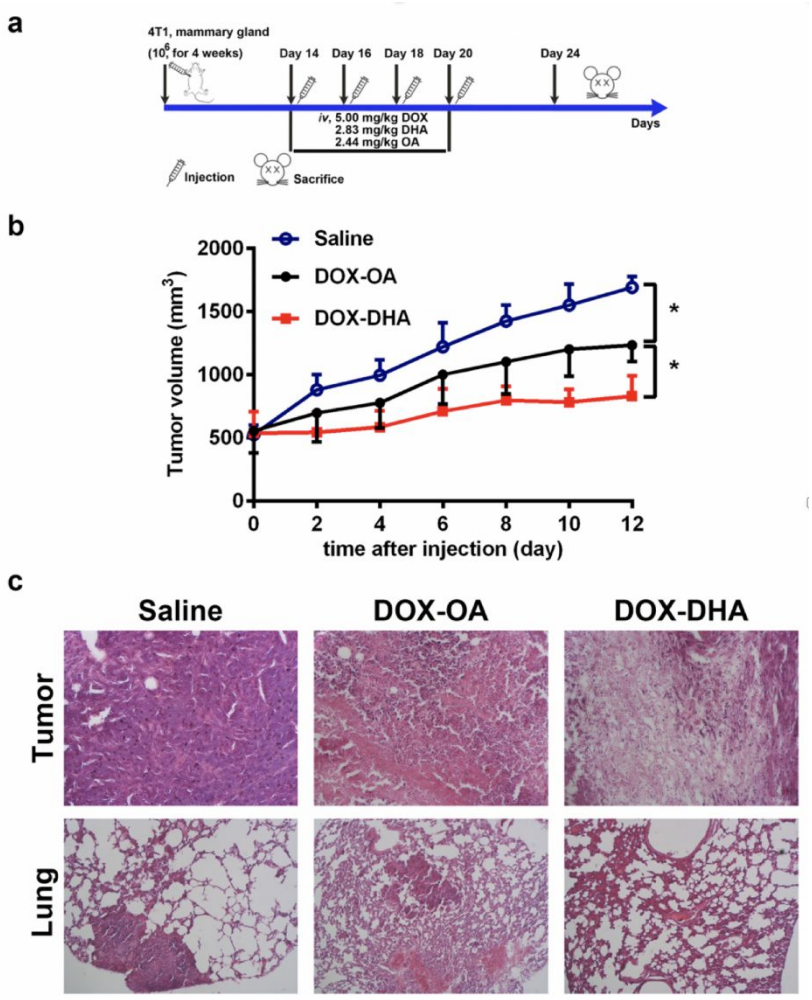

Figure S1. ***In vivo*** **anti-tumor and anti-metastasis effects of various treatments in 4T1 orthotopic breast tumor mice model.** (a) Design and timeline of animal experiment, *iv.*, intravenous. (b) Tumor volumes after treated with saline, DOX + OA, and DOX + DHA for four times with 5.00 mg kg^{-1} DOX, 2.83 mg kg^{-1} DHA or 2.44 mg kg^{-1} OA. Data represent means ± SD (n = 5). (c) Representative images of tumor and lung sections stained for hematoxylin and eosin (H&E). Magnification, 200×. P values were determined by one-way ANOVA with *post hoc* Tukey test and represented using **P* <0.05.

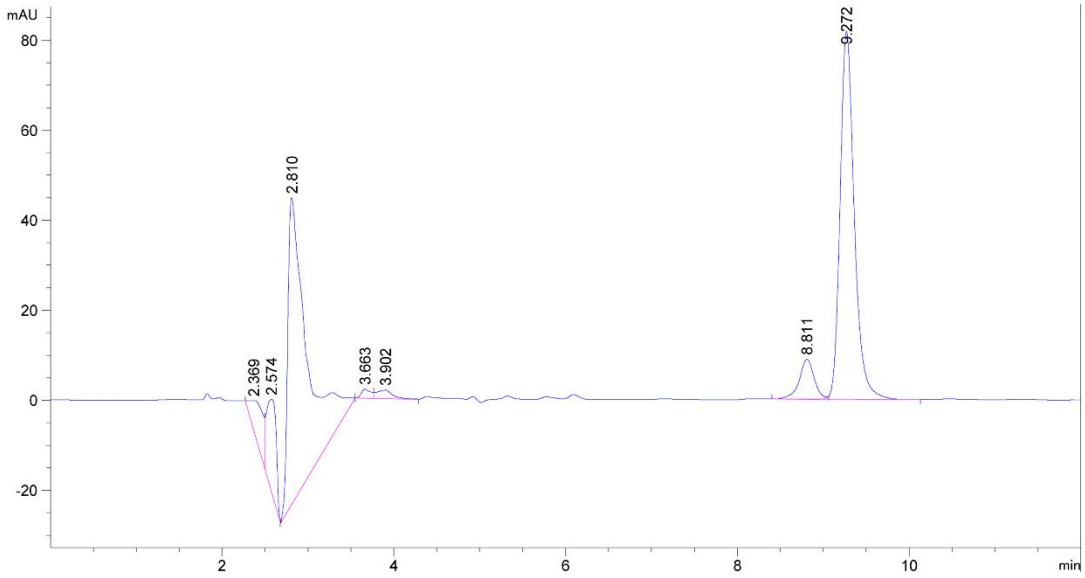

Figure S2. HPLC trace of DHA. The retention time of DHA is 9.3min. Peak area of DHA is 937.5mAU*s.

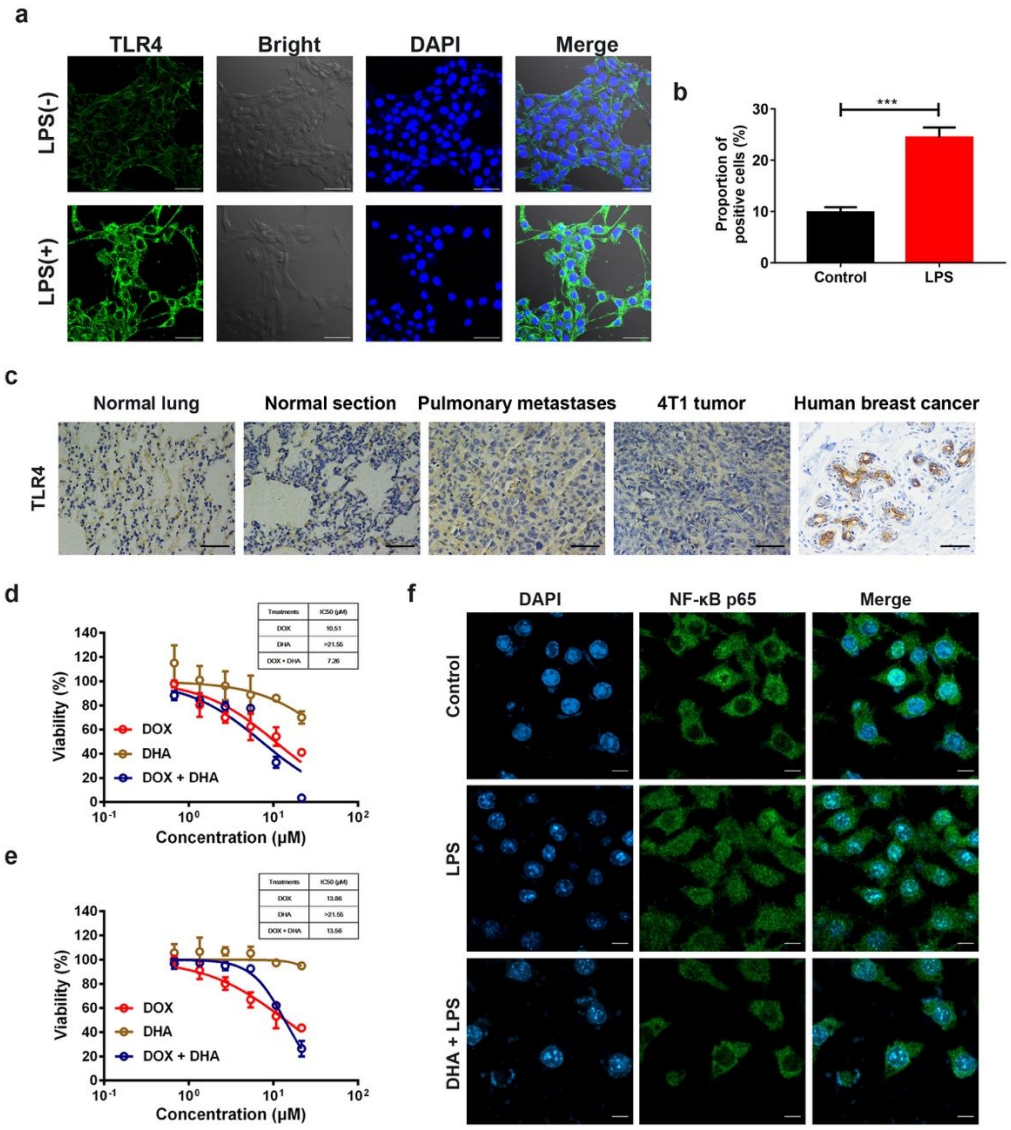

Figure S3. The extensive expression of TLR4, cytotoxic effects of various treatments on 4T1 cells and effect of DHA on NF-κB p65 localization in RAW264.7 cells. (a) Immunofluorescence staining for TLR4 in 4T1 before and after LPS (4 μg mL^{-1}) treatment for 24 h. Scale bars, 40 μm. (b) Quantification of TLR4 on 4T1 cells by flow cytometry. Data represent means ± SD (n = 3). (c) Representative sections of healthy lung of normal mouse, and normal lung area, lung metastasis and tumor sections of 4T1 orthotopic metastasis mouse, and human breast cancer tissue were stained for TLR4. Scale bars, 50 μm. (d) and (e) Dose-response curves of 4T1 cells untreated (d) or treated with 4 μg mL^{-1} LPS pre-stimulation for 24 h (e) against DOX, DHA, and DOX + DHA for 24 h. (f) Representative staining of NF-κB p65 localization was observed by using immunofluorescence confocal. Nuclear translocation of p65 was detected by green in RAW264.7 after LPS (1 μg mL^{-1}, 1 h) stimulus with/without DHA (40 μM, 3 h) pretreatment. DAPI stained nuclei. LPS promoted the rapid nuclear localization of p65, whereas DHA abrogated the translocation of p65 from cytoplasm to nucleus in LPS-stimulated RAW264.7 cells. Scale bars, 10 μm. Data represent mean ± SD (n = 3). *P* values were determined by one-way ANOVA with *post hoc* Tukey test and represented using ***$P < 0.001$.

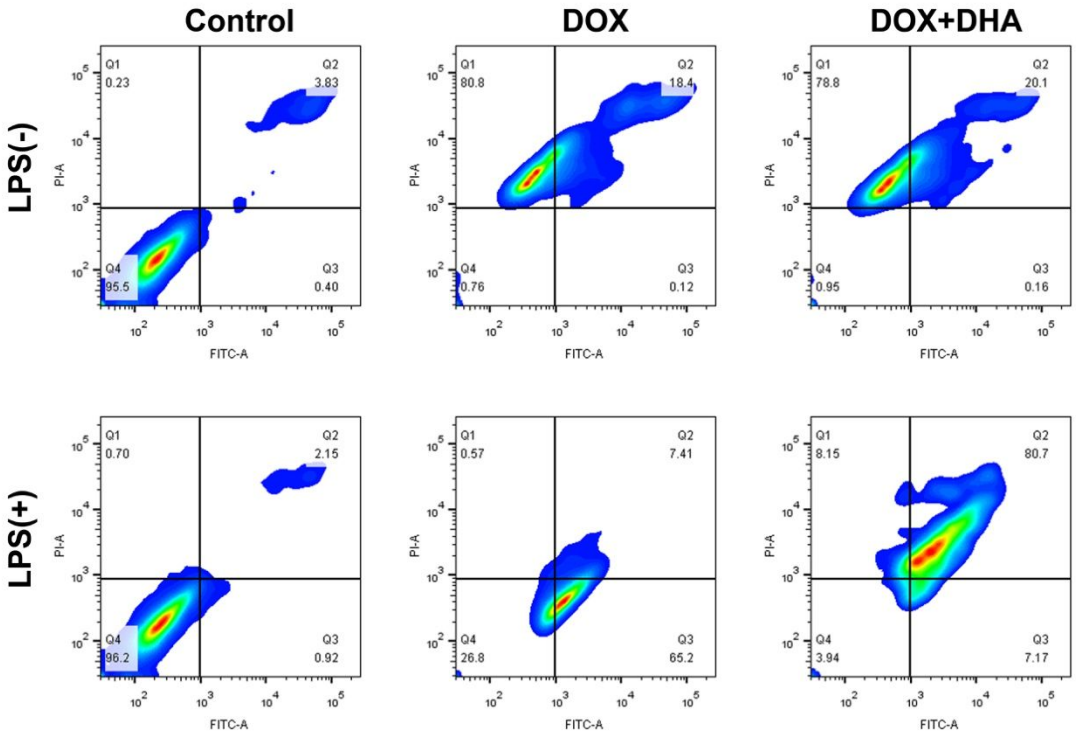

Figure S4. Representative flow cytometry dot plots for Annexin V-FITC/PI staining.

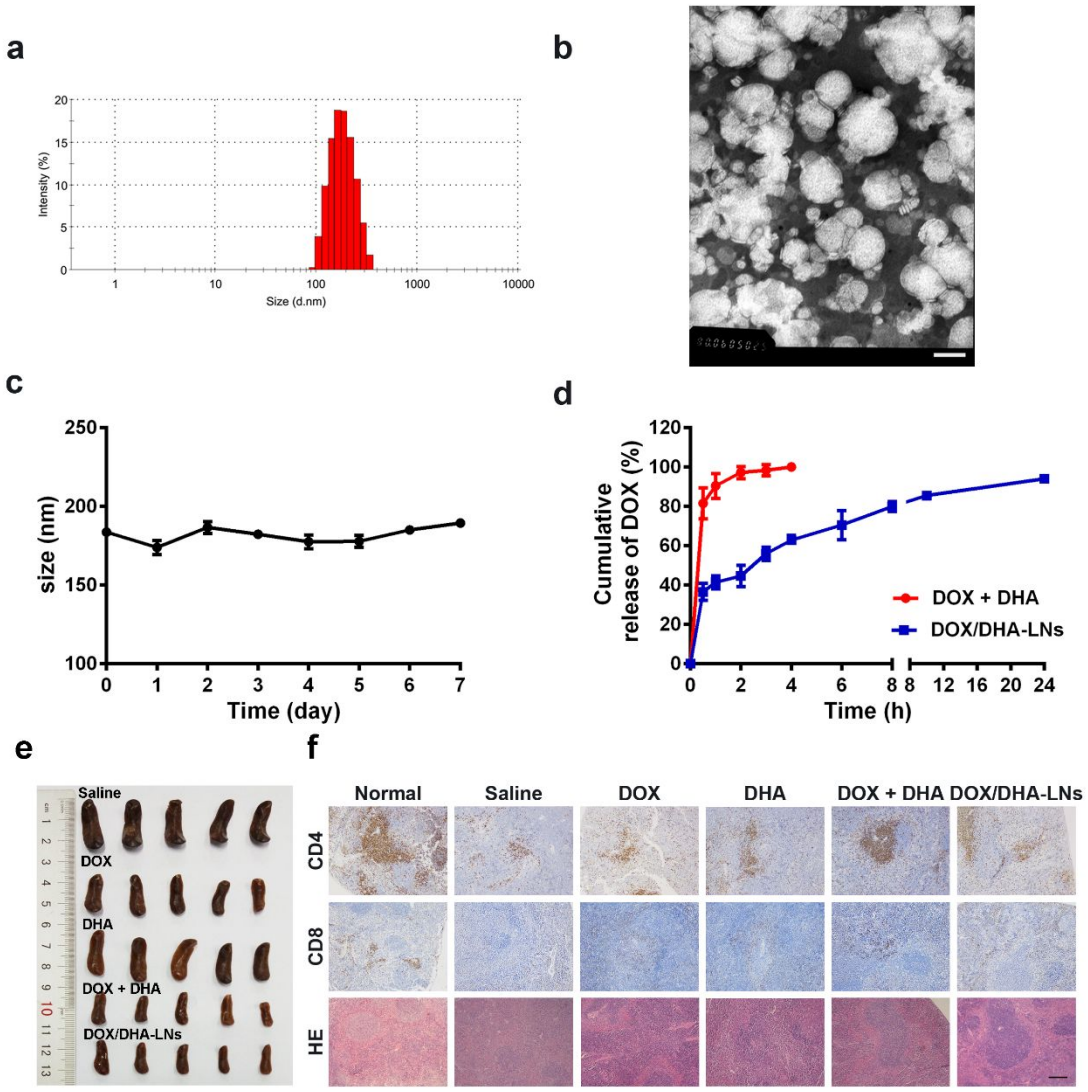

Figure S5. Characterizations of DOX/DHA-LNs and the inhibitory effect of DOX + DHA against splenomegaly. (a) Size distribution of DOX/DHA-LNs determined by dynamic light scattering (DLS). (b) Morphology of DOX/DHA-LNs observed by transmission electron microscopy (TEM). Scale bar, 100 nm. (c) Time-dependent stability of DOX/DHA-LNs under nitrogen protection at 4 °C. (d) In vitro release profiles of DOX from DOX+DHA solution and DOX/DHA-LNs in PBS containing 0.2% w/v Tween 80. Data represent mean ± SD (n = 3). (e) and (f) The images (e) and representative histopathologic examination (f) of spleens from 4T1 orthotopic tumor-bearing mice after treated with saline, DOX, DHA, DOX + DHA, and DOX/DHA-LNs for four times with equivalent doses of 5.00 mg kg^{-1} DOX and 2.83 mg kg^{-1} DHA. Scale bar, 200 μm.

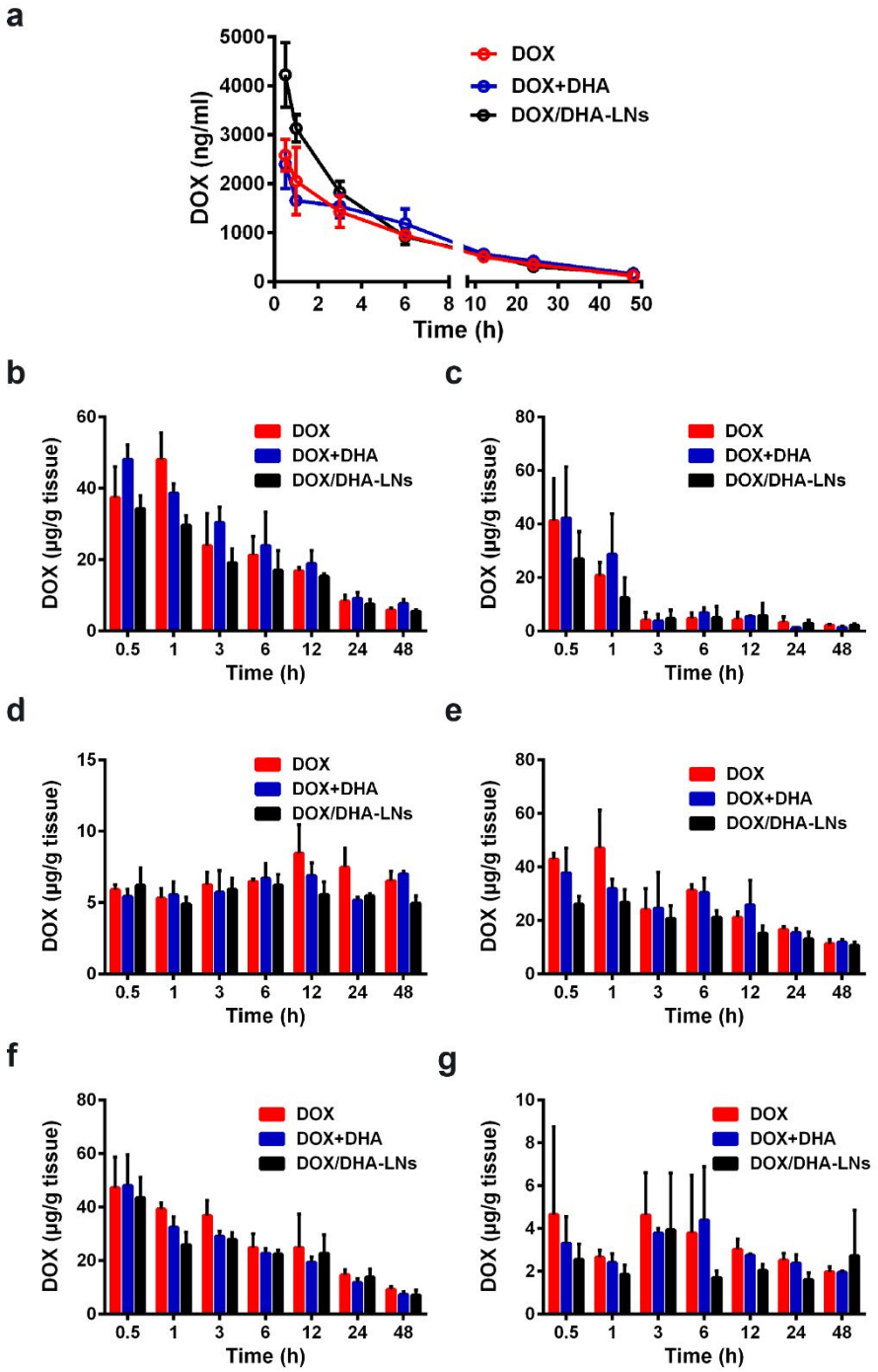

Figure S6. Pharmacokinetics and tissue distribution profiles of DOX in 4T1 tumor bearing mice. 4T1 tumor-bearing mice with tumor size of about 200 mm^3 were intravenously given DOX, DOX + DHA, and DOX/DHA-LNs with 5.00 mg/kg DOX, and the plasma, heart, liver, spleen, lung, kidney, and tumor were collected and stored at -20 °C until analysis. (a) Plasma concentration-time profiles. (b) to (g) Concentration of DOX in heart (b), liver (c), spleen (d), lung (e), kidney (f), and tumor (g). Data represent mean ± SD (n = 3).

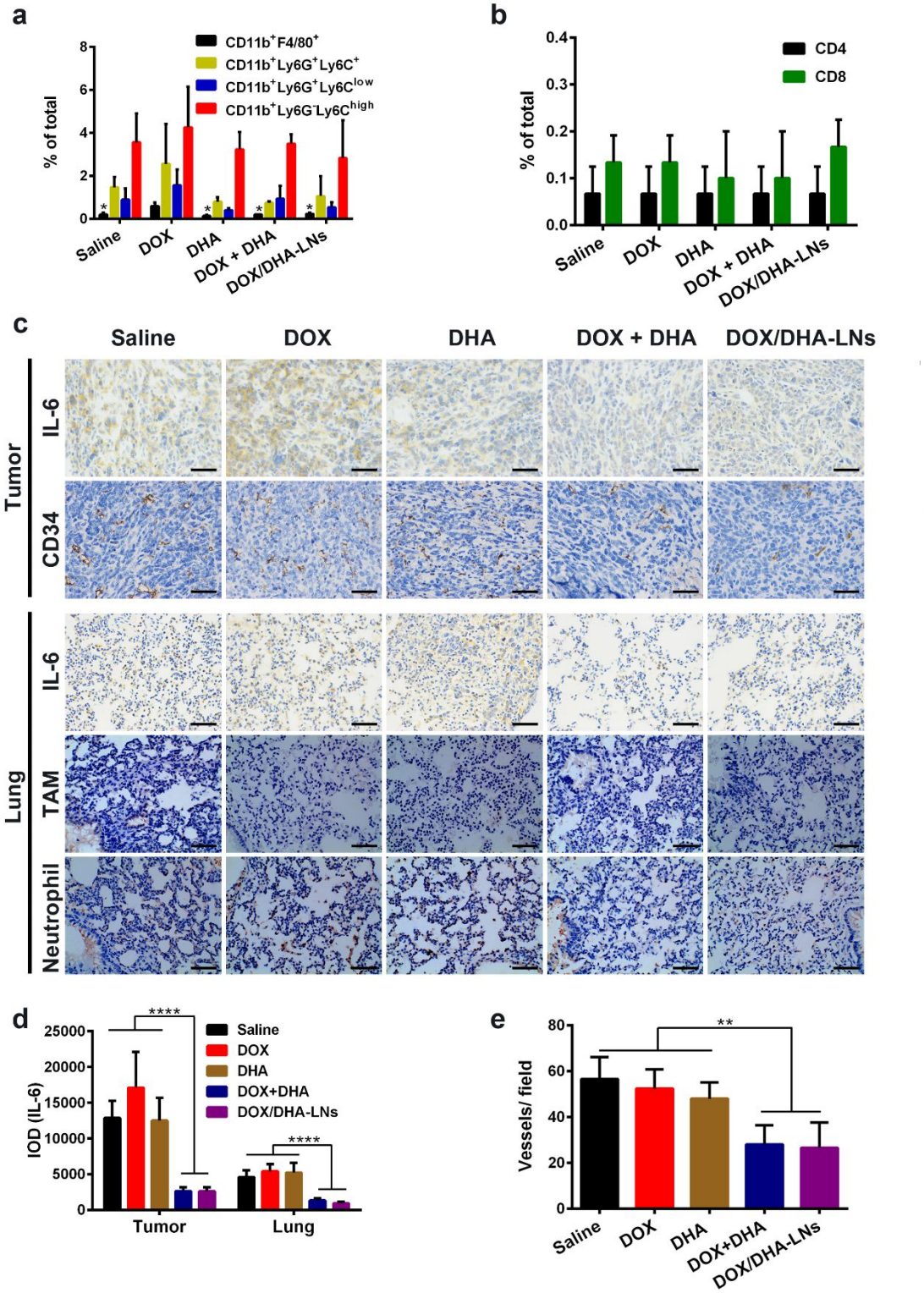

Figure S7. The modulation effect of combination on microenvironment. (a) and (b) The $CD11b^+F4/80^+$, $CD11b^+Ly6G^-Ly6C^{high}$, $CD11b^+Ly6G^+Ly6C^{low}$, $CD11b^+Ly6G^+Ly6C^+$, $CD4^+$ and $CD8^+$ T-cell populations in tumors after treated with saline, DOX, DHA, DOX + DHA, and DOX/DHA-LNs for four times with 5.00 mg kg^{-1} DOX and 2.83 mg kg^{-1} DHA. Each sample was determined by flow cytometry. Data represent mean ± SD (n = 3). *$P < 0.05$, one-way ANOVA with *post hoc* Tukey test. (c) Representative images of tumor sections stained

for IL-6 and CD34, and lung sections stained for TAM, neutrophil and IL-6. Scale bars, 40 μm. (d) and (e) Semi-quantitative analysis for interleukin 6 (d) and blood vessels (e) in tumors or lungs. P values were determined by one-way ANOVA with *post hoc* Tukey test and represented using ****$P < 0.0001$.

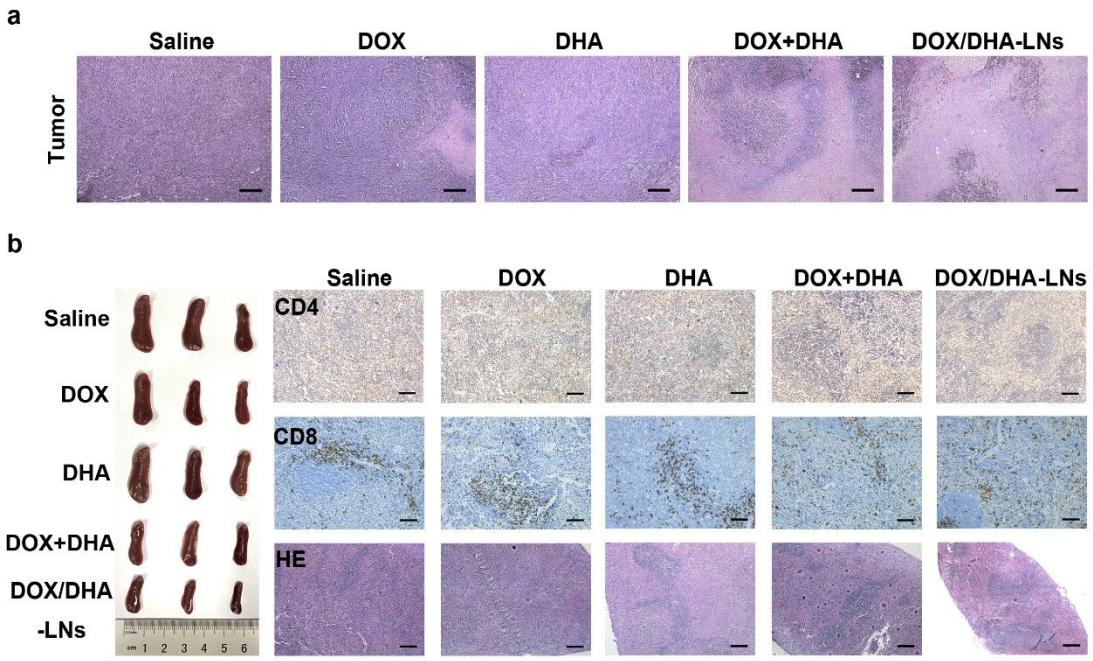

Figure S8. Histological analysis in the postsurgical relapse tumor model. (a) H&E staining of tumor sections. Scale bar, 200 μm. (b) Representative images, CD4, CD8 immunohistochemistry and H&E staining of spleen slices. Scale bar, 200 μm.

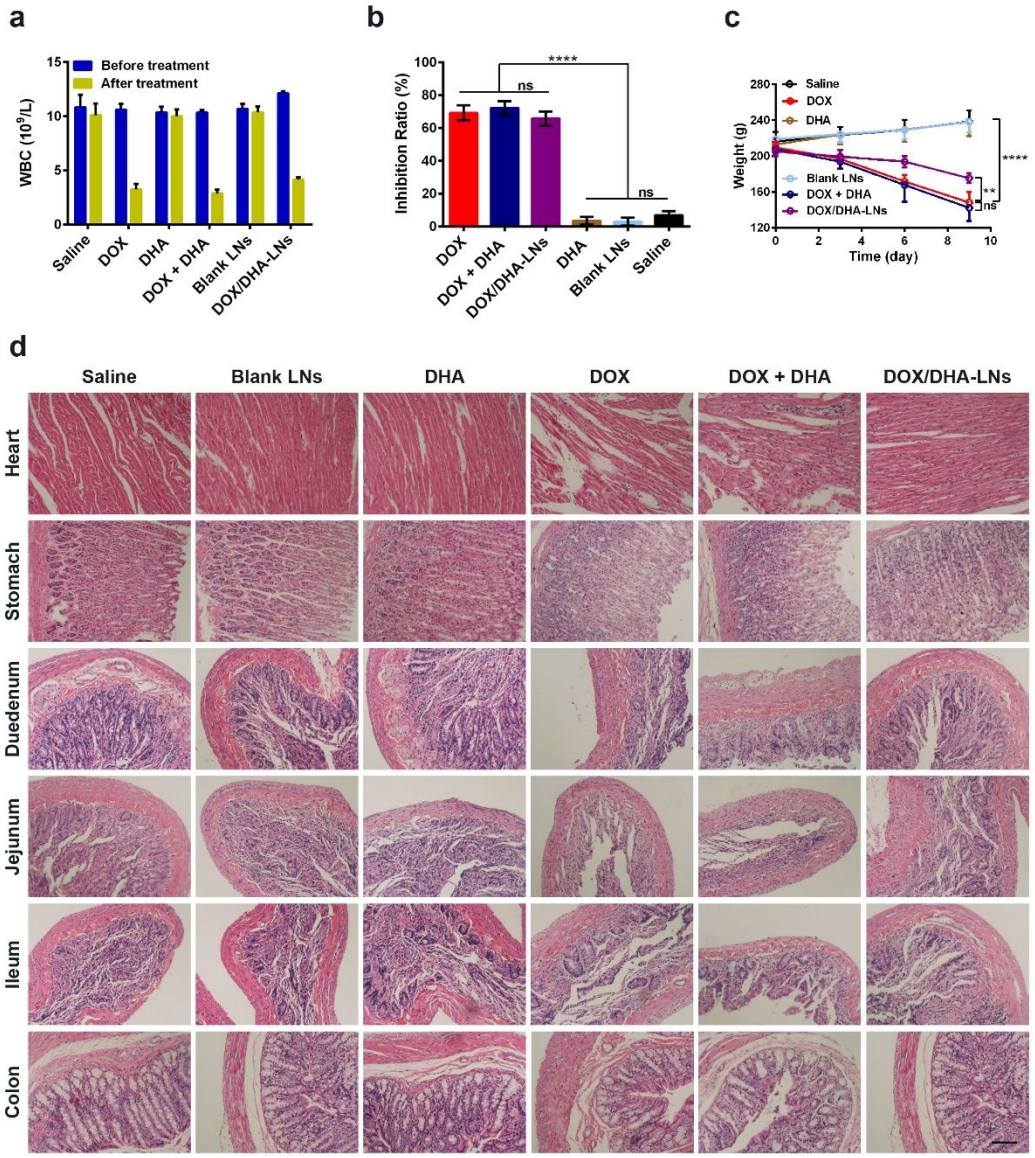

Figure S9. Safety evaluation. To assess safety of various treatments, 30 female Sprague Dawley rats (200 ± 20 g) were randomized into 6 groups and treated with saline, DOX, DHA, DOX + DHA, DOX/DHA-LNs and blank LNs every three days for three times with 6.00 μg/mL DOX or 3.40 μg/mL DHA. All rats were sacrificed at the third day after three treatments, and the plasma, heart, stomach, duodenum, jejunum, ileum, and colon were collected. (a) WBC levels before administration and the end of the experiment. (b) and (c) WBC inhibition ratios (b) and the variation profiles of body weights (c) in each group. (d) Representative heart and gastrointestinal morphology of each group at the end of the experiment. Scale bars, 200 μm. P values were determined by one-way ANOVA with *post hoc* Tukey test and represented using $*P < 0.01$, n.s., not significant.

Table S1. Characterizations of DOX/DHA-LNs. Average particle size, polydispersity index (PDI), zeta potential, and encapsulation efficiency were determined and calculated accordingly. Data represent mean ± SD (n = 3).

Size (nm)	PDI	Zeta potential (mV)	EE_{DOX} (%)	EE_{DHA} (%)
177.6 ± 4.10	0.208 ± 0.012	-6.28 ± 0.61	98.58 ± 1.34	98.75 ± 1.06

Table S2. Summary of pharmacokinetic parameters. Pharmacokinetics parameters were calculated for DOX after intravenous injection of DOX, DOX + DHA, and DOX/DHA-LNs in 4T1 tumor-bearing mice. **P* < 0.05 (DOX/DHA-LNs vs. DOX), data represent mean ± SD (n = 3).

Parameters	DOX	DOX + DHA	DOX/DHA-LNs
AUC_{0-t} (μg/L*h)	24965 ± 2360	27917 ± 817	28688± 1918
MRT_{0-t} (h)	12.63 ± 0.52	13.56 ± 0.83	11.68 ± 0.22
$t_{1/2z}$ (h)	16.24 ± 2.72	17.49 ± 3.86	14.30 ± 6.51
C_{max} (μg/L)	2714 ± 310	2401 ± 501	4170 ± 477*
CL_z (L/h/kg)	0.18 ± 0.02	0.16 ± 0.01	0.16 ± 0.01